

## **The multiparametric statistical analysis of hydrodynamic instabilities based on wavelet preprocessing and neural network classification.**

Studying of Rayleigh-Taylor instability is a fundamental task in hydrodynamics. At the present moment there are two approaches in studying the turbulent flows: a direct numerical calculation using the hydrodynamics equations, and the creation of semi-empirical models for the description of turbulent flows with a small number of parameters. Each of the approaches has a rather restricted field of application of its own. In the present paper a new method of studying the RT-instabilities is demonstrated, which is based on the analysis and generalization of the experimental (calculated) data. Initially the processes are given in the form of a time series of physical quantity distribution pictures. A discrete wavelet-transform of the distribution fields of these quantities resulted in a steady representation: the representation where from a closeness of the initial moments of the process (we mean the closeness by the Euclidean distance between the wavelet-images) follows a subsequent closeness of the later states of the process. Such a specificity of the wavelet-representation allows one to make a probabilistic prediction of the Rayleigh-Taylor mixing by comparing the initial state of the process with the state of the known process.

### **Introduction**

A theoretical study of the turbulent flows is being carried out, at the present time, in two directions. They are a direct numerical simulation (calculation of hydrodynamic equations) and creation of the parametric models based on the statistical averaging of the initial equations, and an application of semi-empirical dependencies for closing the system. The first approach requires time-consuming computer calculations, which restricts its application. In addition, a direct use of the results obtained by that approach would require a precise knowledge of the initial conditions, but such information is not available in most cases of practical importance. In the second approach, one did not succeed in finding a comprehensive description of the turbulent mixing, and the field of application of the existing models is rather limited.

The proposed approach consists in a neuronet analysis of a sufficiently large calculation base, which allows one to make conclusions on the behavior of such processes, and, in a certain sense, to predict the development of hydrodynamic instabilities. As the “learning material a set of two-dimensional simulations of RT-mixing [1] obtained with the NUT code [2] were used. Following the classical theory of the neuronets [3], the creation of a system predicting the development of RT-instability divided into two subtasks: the “search for a convenient representation of physical fields (their sequence sets the processes), and a purely technical problem – the creation of a predictor. In this work a discrete wavelet-transform of the density fields was used to form the input vectors of a neural network. The advantages of such a representation were discussed in [4,5].

Below we give a description of the learning sample, present a scheme of the calculated data, and create a predictor. The prediction results obtained with the predictor will be compared with the real calculated pictures.

### **Calculations performed by the NUT program**

The geometry of a system calculated in a Rayleigh-Taylor problem is shown in Fig.1 (the dimensions are in mm). The system consists of two rectangular regions (OABC and OCDE), which are separated by a horizontal plane (contact boundary).

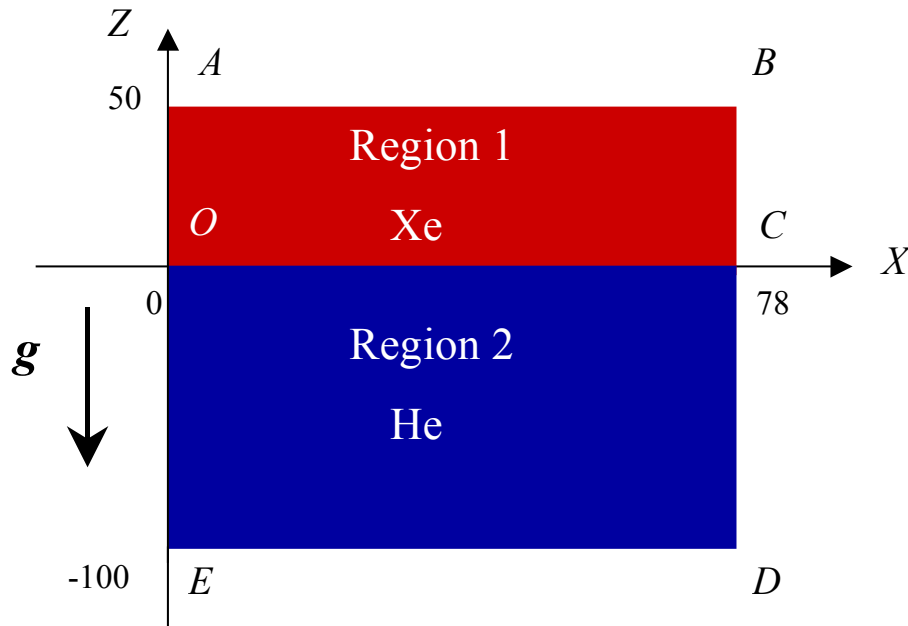


**Fig. 1. The system geometry in the Rayleigh-Taylor problem calculations.**

External field of the gravitational force is applied normal to the contact boundary with the free fall acceleration  $g = 10^4 g_0$  directed downward against the vertical axis  $OZ$ , where  $g_0$  is the free fall acceleration near the Earth surface. The heavy gas xenon (Xe) lies in the upper region, and the light helium (He), in the lower. A non-flow condition is set on the upper (AB) and lower (DE) boundaries of the system (vertical speed component is equal to zero). On the lateral walls (AE and BD), a periodic boundary condition is set.

To describe the thermodynamic properties of gases one used the ideal gas equation-of-state in the form of  $p = \frac{R}{\mu} \rho T$ ,  $\varepsilon = \frac{1}{\gamma - 1} \frac{R}{\mu} T$ . The initial distributions of pressure and density correspond to the isentropic configuration:

$$\rho_i(z) = \frac{p^{1/\gamma}}{B_i}; \quad p_i(z) = \left( \tilde{p}_0 - \frac{\gamma - 1}{\gamma B_i} g z \right)^{\gamma/(\gamma - 1)},$$

where  $\tilde{p}_0 = p_0^{1/\gamma}$ ;  $B_i = \frac{T_0}{M_i P_0}$ ,  $M_i$ , the mass of the  $i$ -th gas particle,  $T_0 = 300K$ , and  $p_0 = 0.5$  standard atmosphere.

The calculations were being taken up to the moment  $t = 1250 \mu s$ . Within every  $\Delta t = 50 \mu s$  the set of the physical values had been recorded:

- |   |  |
|---|--|
| 1. Position of the contact boundary -             | $z(x)$   |
| 2. Density field -                                | $\rho(x, z)$   |
| 3. Pressure field -                               | $P(x, z)$  |
| 4. Fields of the speed components -               | $u(x, z), w(x, z)$   |
| 5. Fields of the pulse components -               | $p_x(x, z), p_y(x, z)$   |
| 6. Field of the volume specific internal energy - | $e(x, z)$  |
| 7. Curl of velocity -                             | $\Omega(x, z) = \frac{\partial u}{\partial z} - \frac{\partial w}{\partial x}$ , |

of which only the density will be considered furthermore. The calculations differ from each other by the shape of initial perturbation of the contact boundary only. It actually determines a further dynamics of the mixing.

In this work, the database is used which consists of 32 processes calculated by the NUT code. The processes had been set by the pictures of density distribution in 26 moments of time. Figure 2 illustrates some states of one of the processes. The digits mark the time moments, to which the given states correspond.

The initial perturbation  $s$  of the interface surface, in the studied processes is set by six harmonics,  $s = \sum_k a_k \cos(\frac{2\pi kx}{L} + \varphi_k)$ , where  $k = 2,3,5,7,11,13$  and  $L$  is the frame width (length of the segment OC, Fig.1). The amplitudes of harmonics  $a_k$  are the same in all the calculations and obey the condition  $a_k \frac{2\pi k}{L} = 0.5$ . Thus, the initial perturbations differ by the choice of the harmonic phases,  $\varphi_k$ , only. The phases may have only one of the eight values:  $\frac{\pi}{4}n$ , where  $n = 0,1,\dots,7$ , and are chosen randomly.

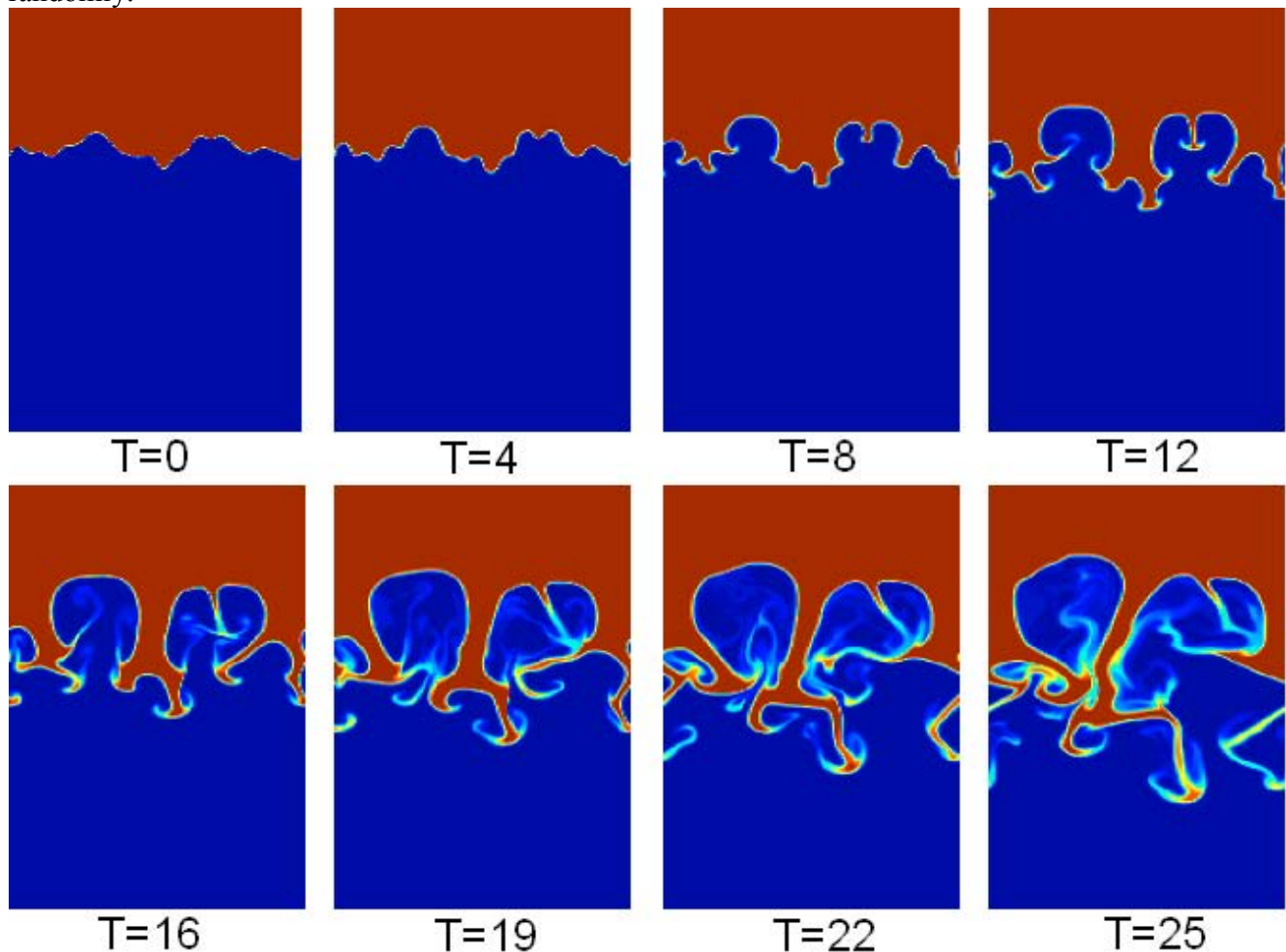


**Fig.2. Evolution of density of the two-dimensional RT-mixing process.**

To increase the learning sample the initial database of the processes was expanded by mirror reflection of the density distribution pictures with relation to the vertical axis and their parallel transfer along the horizontal axis. The latter becomes possible due to the periodicity of boundary conditions at the sidewall. As a result, 640 processes were involved in the processing procedure.

**Consideration of spatial information by means of wavelet-coding of the initial fields.**

The pictures of density distribution are set in the form of the density matrices placed in the cells of two-dimensional mesh. In further analysis, it is necessary to introduce a certain “measure of convergence” of the pictures, which is a value characterizing numerically a degree of closeness of the physical properties of two distributions. One can represent the pictures as the parameter vectors, and the “measure of convergence” of two density distributions determine as, for example, an Euclidean distance between the respective vectors. Evidently, it is not physically correct to choose as the parameters of such vectors the initially determined numerical characteristics of the density in the mesh cells. The distance between the pictures, as can easily be seen, is unstable in respect to small spatial displacements. To eliminate that difficulty one has to transform initial information into another representation, which is not very sensitive to spatial displacements. In addition, if one succeeds in finding the representation, in which a similarity of the initial states causes a similarity of the final states, one might predict the processes of the RT mixing.

Thus, the aim of the work is the search for such a transformation of the initial density fields, which leads to a steady representation, where from a closeness of the initial moments of two different RT-mixing processes (closeness by the Euclidean distance) follows a subsequent closeness of those processes in the given representation. As a first step towards a formation of such a representation one can apply, for the density fields, a two-dimensional discrete wavelet-transform [6]. The wavelets are the functions, which are well localized in space, owing to which they define spatial distributions of a studied value in different scales. Unlike a classical Fourier-base where the basic functions differ (in one-dimensional case) by one parameter of the frequency, the functions of the wavelet-base have two parameters. They are the scale parameter  $a^{-1}$ , which determines the size of a wavelets (being considered as the analogue of the Fourier-base frequency) and the characteristic scale of the studied structures, and the displacement parameter  $b$ , which is responsible for the wavelets  $\psi\left(\frac{x-b}{a}\right)$

occurring in a certain region of space. By choosing values of the parameters  $\{a_n, b_m\}_{n,m}$  one can obtain a full orthonormal system of functions leading to the so called discrete wavelet-transform. By applying the discrete wavelet-transform to 2D density distribution functions  $\rho$  we use the 2D wavelet-base, whose functions differ, respectively, by four parameters

$$\rho(x, z) = \sum_{i=1}^N \langle \rho | \psi_i \rangle \psi_i = \sum_{i=1}^N c_i \psi_i .$$

The expansion coefficients  $\{c_1, c_2, \dots, c_N\}$  make the wavelet-image of the initial function  $\rho$  and determine it unambiguously. As a result, each field, which determines the corresponding moment of time, will be set by the vector-column of the wavelet-coefficients  $\{c_1, c_2, \dots, c_N\}$ . The density fields represented in such a way may be treated as points in the  $N$ -dimensional space, on the axes of which the values of the wavelet-coefficients are plotted. As a result, a point in space will characterize the state of the process at any moment of time, and a broken line will describe the process as a whole.

Such a space has large dimensionality, which makes a further analysis difficult. First, the purely computational difficulties arise which are connected with a necessity to process large amount of data. Second, it is known that at a neuronet data treatment the error of the neuronet increases with growth of dimensionality of the input vector [3]. Thus one has to decrease the dimensionality of the data even by a certain loss of information. The first roughening consists in neglecting the small-scale wavelet-coefficients, which is actually a deterioration of resolution of distribution of a physical value. By assuming that small structures of the wavelets had no essential influence on the course of the process, such roughening would not produce any considerable loss of information for our problem during the time of our calculations.

To perform a further data compression one use the method of the principal linear components, which is the linear transformation of the coordinates, where the first principal component lies along the greatest data dispersion direction, the second one finds the second by the value of dispersion direction, and so on. To get the matrix of this transformation calculate the mean vector and the data covariant matrix:

$$\bar{\mathbf{c}} = \frac{1}{P} \sum_{\alpha=1}^P \mathbf{c}^\alpha, \quad \Sigma_{ij}^C \equiv \frac{1}{P-1} \sum_{\alpha=1}^P (c_i^\alpha - \bar{c}_i)(c_j^\alpha - \bar{c}_j),$$

here  $P = 640 \times 26$  is a complete number of the density distribution pictures. Further the problem on the proper values is solved:

$$\sum_j \Sigma_{ij}^C U_{jk} = \lambda_k U_{ik}$$

The linear transformation  $PC_i = (c_k - \bar{c}_k)U_{ki}$  turns all the inputs into uncorrelated zero mean values.

One may neglect the low-dispersion (i.e. regular) components by leaving the first  $K$  coordinates (where  $K \ll N$ ), the main part of the information being preserved. Such compression allowed one to decrease the dimensionality of the space by hundred times, in our case. The linear combinations of the wavelet-coefficients will serve as coordinates in a new representation.

Figure 3 illustrates a) an initial picture of 130x250 pixels; b) a picture reproduced after a compression up to 200 components; c) up to 40 components; d) up to 17.

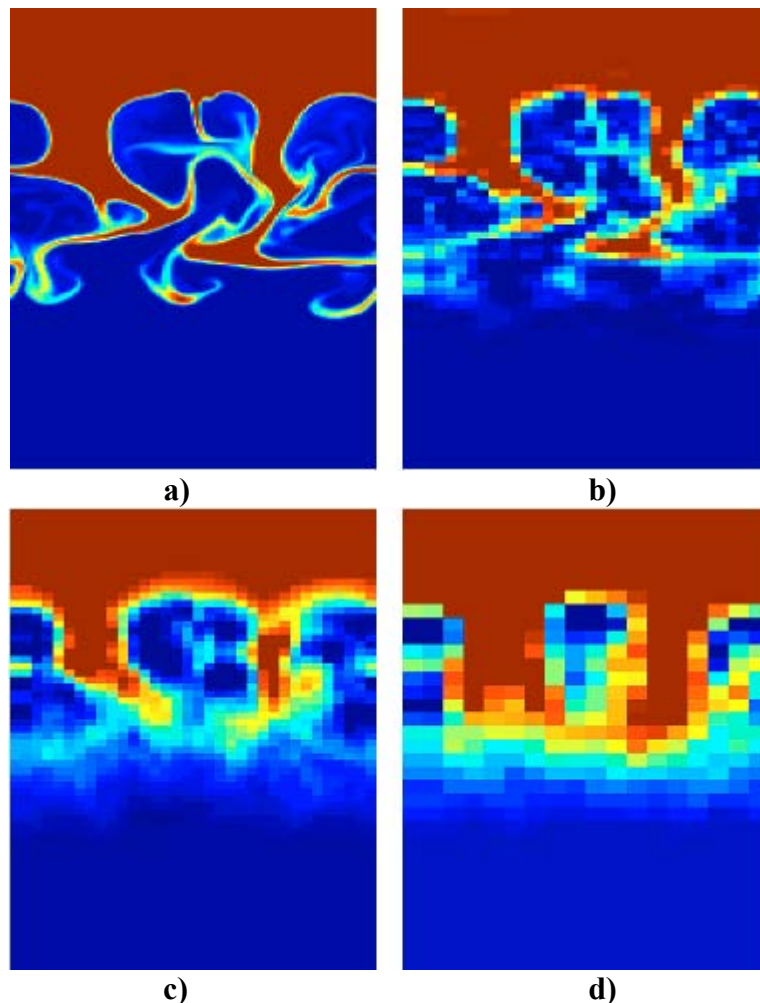


**Fig.3. Density field reconstructed after the dimensionality decrease by the method of principal components.**

### Filters of direct transform

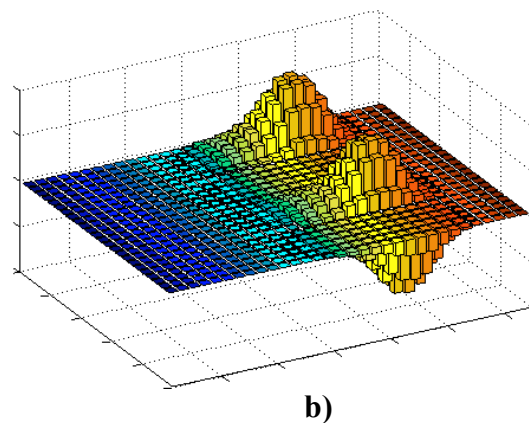
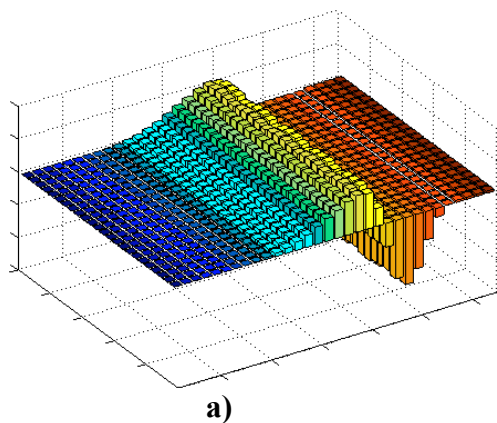
As a result of a transform, each time moment of each of the processes will be given by a set of values of the principal components  $\{PC_1, PC_2, \dots, PC_N\}$ . The procedure consists of two successive steps: the wavelet-expansion of density fields and multiplication of wavelet coefficient vectors by the turning matrix. By combining these two procedures into a one it is possible to get the filters, which, under the convolution with the density fields, give the values of the corresponding principal components.

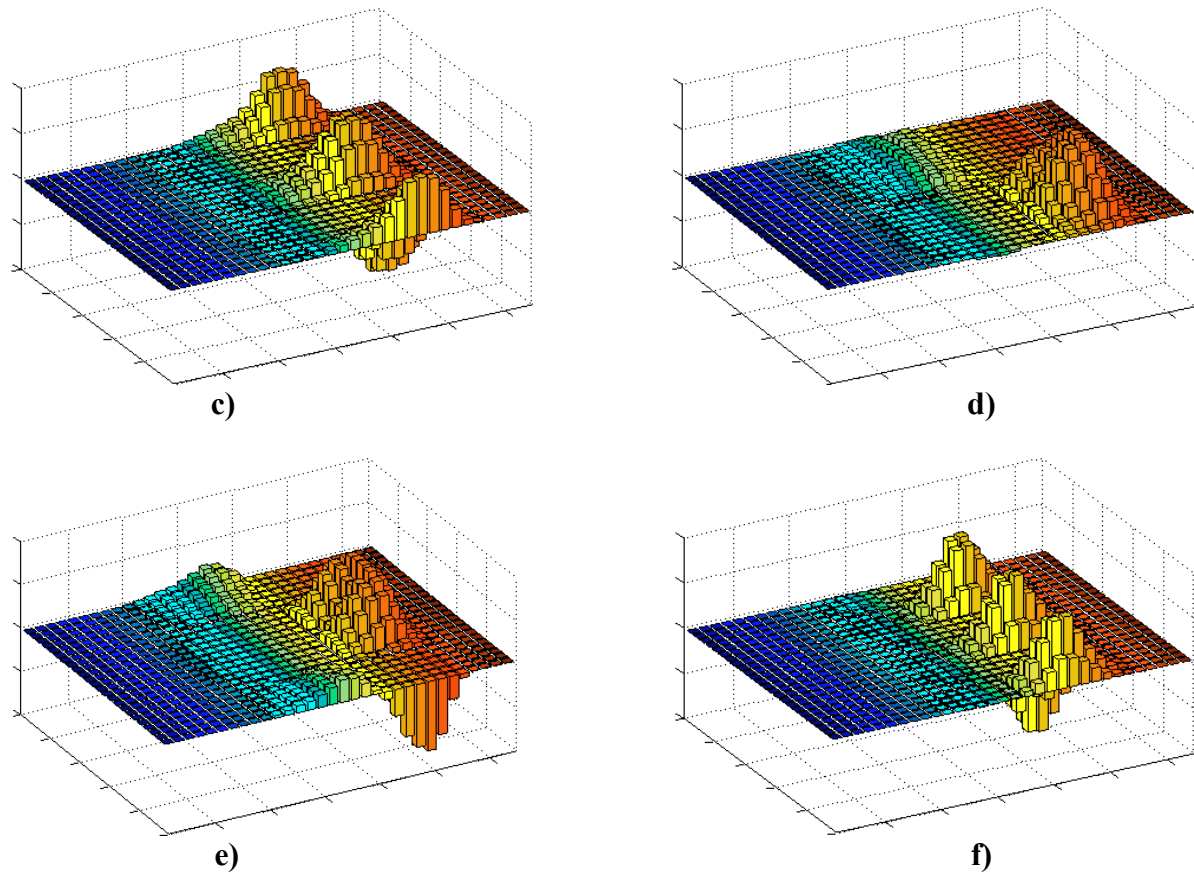
$$c_i^\alpha = \langle \rho_\alpha | \psi_i \rangle \quad PC_k^\alpha = \mathbf{cU}_k - \bar{\mathbf{c}}\mathbf{U}_k = \sum_{i=1}^N c_i^\alpha \langle \psi_i | \psi_i \rangle U_{ik} - \bar{\mathbf{c}}\mathbf{U}_k = \langle \rho_\alpha | FPC_k \rangle - const_k$$

Here it is taken into account that  $\rho_\alpha = \sum_{i=1}^N c_i^\alpha \psi_i$  and the filters of the principal components

$FPC_i = \sum_{i=1}^N U_{ik} \psi_i$  are introduced. Some of them are presented below (see Fig. 4).

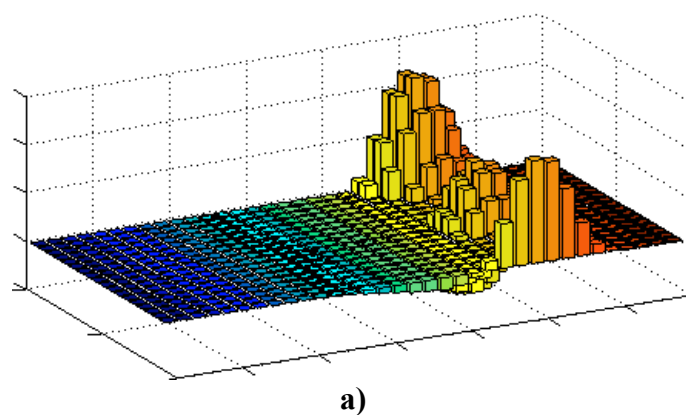
In [5] it was shown that the value of the first principal component (FPC) strongly correlate with such physical quantities as the time, the width of the mixing zone, the intruded mass, etc. This could be expected from the outward appearance of the FPC filter. At the initial time moment practically all the mass is concentrated in the upper part of the frame (Fig. 1), where the filter matrix elements have strongly negative values (Fig.4a), and, correspondingly, for the early stages of the process the FPC value will have large modulo negative value. As a heavy liquid flows into the region initially filled with a light liquid, the value of the FPC will grow. The filter for the second principal component (SPC) differs from zero only in the vicinity of the phase interface (Fig. 4b). Here the filter has two humps and two troughs alternate along the horizontal axis. The peaks of the humps and troughs are located approximately above the interface at zero moment of time. In a vertical direction the coefficients of the SPC make half-oscillation. So, one may conclude that the SPC is sensitive to the flow of a heavy substance in a horizontal direction. The filter for the third principal component may be treated as the filter for the SPC shifted along the horizontal axis by 1/8 of the frame. Thus we have two filters of the same scale sensitive to the circulation of a heavy liquid in a horizontal direction: an antisymmetric filter and a symmetric one. Then go the filters, which have the form of an uneven and even functions relative to the vertical median of the frame. They may be treated as a product of functions oscillating in  $Z$  (like FPC) and  $X$  (like SPC) directions, and their effective “wavenumbers” increase with their ordinal number. The subsequent components are responsible for the heavy liquid flow of a smaller scale: the filters have a larger number of humps and troughs.





**Fig.4. Filters of principal components**

The filters corresponding to first (Fig. 5a) and second (Fig. 5b) principle components of Daubechies2 representation are introduced below. Taking a linear combination of these filters, one can obtain the filter, whose meaning is analogous to the first principle component of Daubechies1 representation. This fact is the evidence for the direction, along which the “age of a process changes, to lie somewhere in the vicinity of the plane formed by first two principle components.



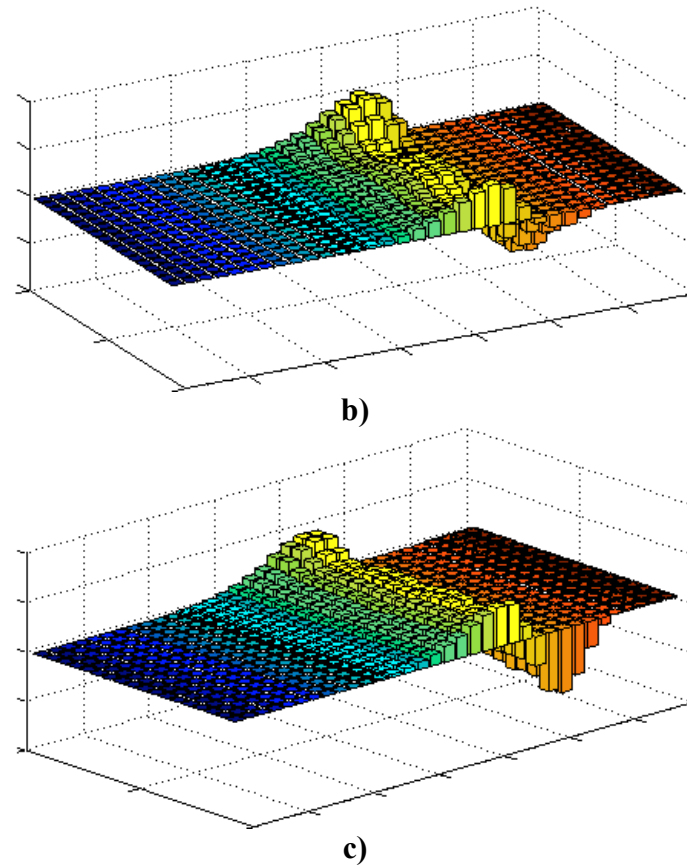


**Fig.5 Filters of the first (a) and the second (b) principal components for Daubechies 2 representation and filter for linear combination of first and second components (c).**

**Predictor**

Let us perform clusterization of the initial states (the states corresponding to zero moments of time), rigidly fixing the number of clusters. In this case the processes are distributed among the clusters in a certain ratio  $N_1, N_2, \dots, N_I = \{N_i\}_{i=1}^I$ , where  $I$  is the number of clusters. Taking the same number of clusters let us perform clusterization of the states at the time moment  $t$ . Let there be  $N_i$  processes in the  $i$ -th cluster at the initial moment of time; at the time moment  $t$  these processes are distributed in a certain way over the clusters  $N_{i,1}(t), N_{i,2}(t), \dots, N_{i,I}(t) = \{N_{i,j}(t)\}_{j=1}^I$  (here

$\sum_{j=1}^I N_{i,j}(t) = N_i$ ). The probability that the process initially placed in the  $i$ -th cluster will fall within the

cluster  $j$  at the time moment  $t$  may be estimated as follows:  $P_{i,j}(t) = \frac{N_{i,j}(t)}{N_i}$ . The scheme of the

predictor is depicted on Fig. 6. As a result, if one defines which cluster includes the new unknown process at zero time moment, then, with the probability  $P_{i,j}(t)$ , one can define its location at the time moment  $t$ . As a prediction one can take the states of the processes of a learning sample located in the most credible area of a phase space. At the addition of new processes to the database the transition probabilities are to be subject of correction.

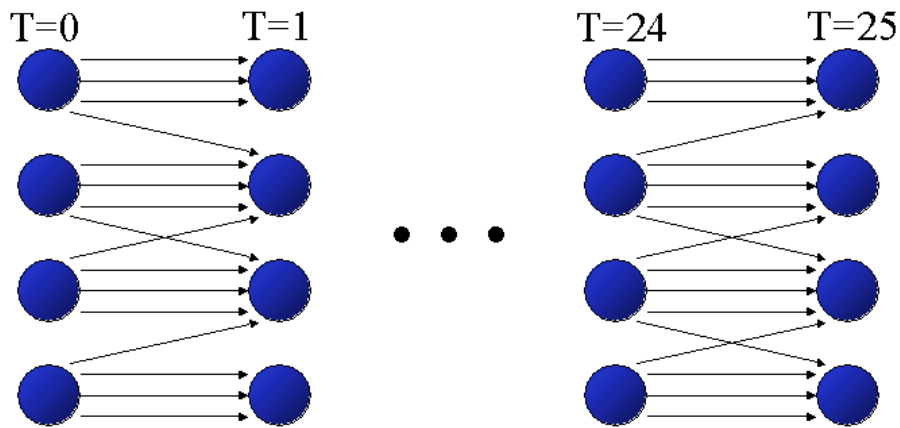


**Fig.6 Scheme of a predictor**

Figure 7 (top) shows the initial state of the tested process and its state at 25-th moment of time received from direct calculation. Figure 7 (bottom) shows two pictures of density distribution, which correspond to the states of the process in the learning sample located in the cluster indicated by the predictor. As seen from the figure, the main features specific to density distribution pictures from the given space area are also present in the studied process.

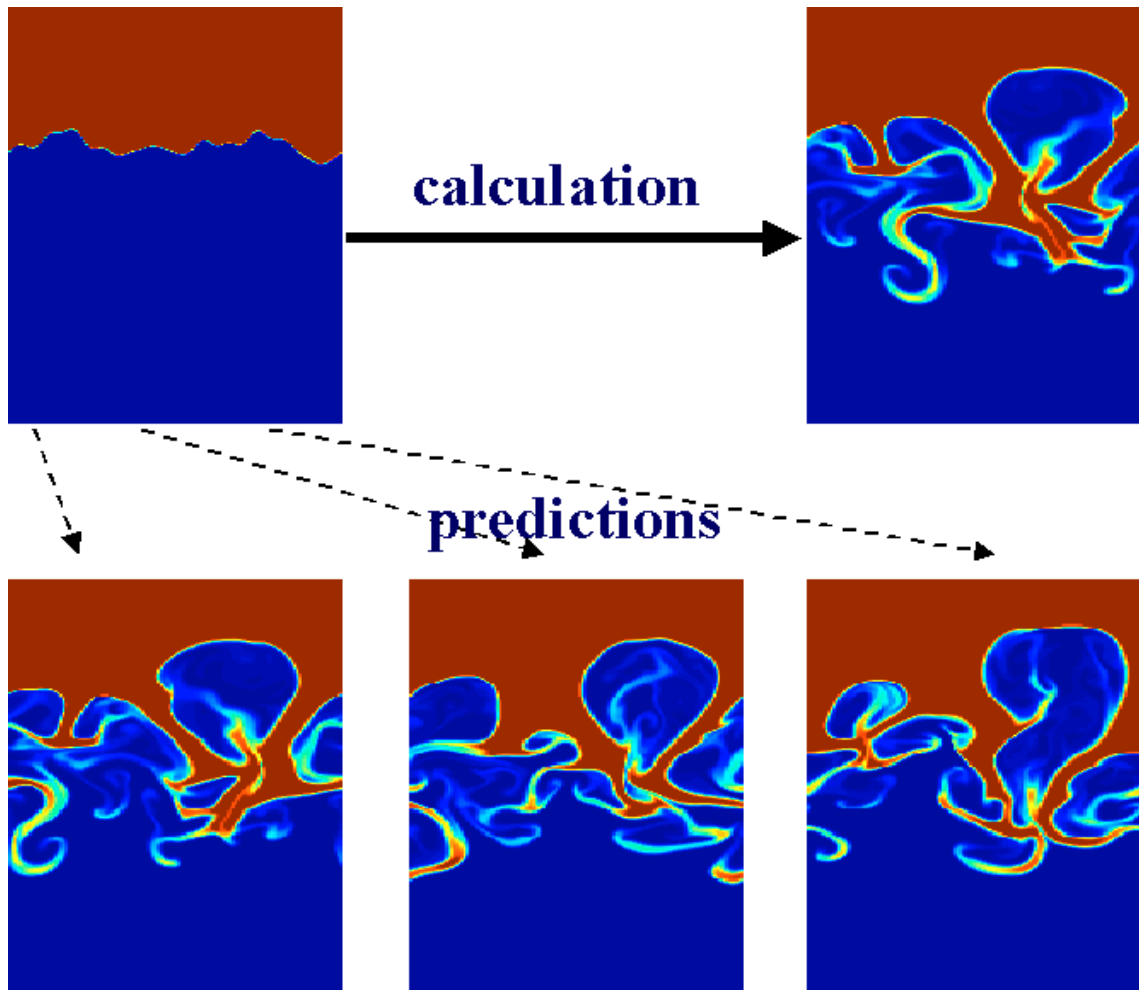


**Fig.7. The results of the predictor. The top pictures illustrate the density distribution for the initial and final states of the tested process. The bottom pictures – the predictor results.**

## Conclusion

The obtained results:

- The method of principal components revealed the value (FPC), which has the physical meaning of the process “age”. Its distribution in the wavelet component space is strongly correlated with the distribution of such values as the elapsed time, the mixing zone width, potential energy, intruded mass, etc.
- The subsequent principal components trace the flow of liquid in a horizontal direction at different scales. Here the less informative components (with smaller data dispersion) are responsible for more small-scale mixing.
- The software module is developed which predicts, by initial state of a process, the most probable area in the phase space to contain the state of this process at later time.

The results obtained indicate a possibility in principle to create, with the help of neural networks, of the semi-empirical models for the prediction of turbulent mixing.

## References

1. G. Taylor, Proc. Roy. Soc. London A201, 192, (1950).
2. V.F. Tishkin, V.V. Nikishin, I.V. Popov, A.P. Vavorsky, Mathematical Modelling, 7(5), 15, (1995) (in Russian).
3. C.M. Bishop, “Neural Networks and Pattern Recognition”, Oxford Press, (1995).
4. A.S. Nuzhny, V.B. Rozanov, R.V. Stepanov, S.A. Shumsky «Analysis of Rayleigh-Taylor Instability by Nonlinear Statistics Methods for the Tasks of Laser Thermonuclear Fusion» XXVII European Conference on Laser Interaction with Matter.
5. A.S. Nuzhny, V.B. Rozanov, R.V. Stepanov, S.A. Shumsky “Study of Rayleigh-Taylor instability in inertial laser fusion (ILF) problem and comparison of different calculation methods by wavelet coding of the initial physical fields and their neuronet processing.”, preprint № 12 LPI 2004.
6. I. Daubechies. “Ten lecture on Wavelets. CBMS-NSF Regional Conf. Series in Appl. Math., Vol. 61. Society for Industrial and Applied Mathemedics, Philadelphia, 1992.